

Cardiac Ultrastructure in Streptozotocin-Induced Diabetic Rats

Passara Lanlua, Ph.D.*, Phatiwat Chotimol, M.Sc.*, Sirinush Sricharoenvej, Ph.D.*, Sani Baimai, M.Sc.*, Sitha Piyawinijwong, Ph.D.*

*Department of Anatomy, Faculty of Medicine Siriraj Hospital, Mahidol University, Bangkok 10700, Thailand.

ABSTRACT

Objective: To examine the alterations of four cardiac chambers in the streptozotocin (STZ)-induced diabetic rats by using light and transmission electron microscopies

Methods: Eleven STZ-induced diabetic and six control adult male Sprague-Dawley rats were applied. After the induction for 24 weeks, all heart chambers were proceeded with histological and ultrastructural techniques.

Results: In the diabetes, swollen endothelial and mesothelial cells laid on thick basal lamina, and their cytoplasm comprised numerous pinocytotic vesicles, vacuoles, and dilated rER. The subendocardial and subepicardial layers were enlarged with accumulations of collagen fibrils. Both cardiac myocytes and Purkinje fibers became hypertrophy. The interstitial fibrosis, contraction band necrosis, and infiltrations of lymphocytes and macrophages were observed in some areas of myocardium. The myocardium of the left ventricle showed interstitial hemorrhage. In both cardiac myocytes and Purkinje fibers, the arrangement of sarcomere was irregular with lost myofilaments. Moreover, swollen mitochondria with disrupted cristae were examined and increased in number. The number of specific atrial granules decreased in the atrial cardiac myocytes. Increased lipid droplets and myelin figures were seen in the myocytes. The intercalated disc was disrupted in some portions. The capillary lumen was narrowed due to swollen endothelial cells with thick basal lamina.

Conclusion: DM causes numerous cardiac alterations in all three layers of four chambers. This study provides an important basic knowledge for understanding the pathological changes and options for further therapeutic treatment of cardiac complications in the diabetic patients.

Keywords: Heart, diabetes mellitus, streptozotocin

Siriraj Med J 2012; 64 (Suppl 1): S49-S53

E-journal: <http://www.sirirajmedj.com>

INTRODUCTION

Cardiovascular diseases are more prevalent in the patients with diabetes mellitus (DM).¹ Many researchers have ultrastructurally investigated the cardiovascular effects of DM. Most ultrastructural studies in the diabetic hearts have been focused on only the ventricular myocardium.²⁻⁴ while either atrial chambers or three layers of cardiac wall; endocardium, myocardium, and epicardium, have not been fully elucidated. Therefore, the objective of present study was to examine the alterations in all cardiac chambers of the streptozotocin (STZ)-induced diabetic rats by using light microscopy (LM) and transmission electron microscopy (TEM).

MATERIALS AND METHODS

Animal Preparation

Seventeen male Sprague-Dawley rats (National

Laboratory Animal Center, Mahidol University, Salaya, Nakonpathom, Thailand, 5-8 weeks old, 200-270 g) were randomly separated into control (n=6) and diabetic (n=11) groups. The Mahidol University Council's Criteria for Care and Use of Laboratory Animal were followed to perform in this study. A week after the arrival, each animal was fasted at least 6 hours, and the glucose concentration in urine was determined by using the urinalysis control strips (Diabur-Test 5000, Roche Ltd., Germany). The results of the urine glucose concentrations were 0 mg/dL; therefore the animals can be applied in the experiment.

Induction

In the DM (n; LM=5, TEM=6), a single dose of STZ (60 mg/kg body weight; Across Organics, Janssen Pharmaceutical, Belgium) in the citrate buffer at pH 4.5 was injected intraperitoneally into each rat. In the control group, the rats (n; LM=3, TEM=3) were injected intraperitoneally with the same amounts of the citrate buffer. In every morning, the urine glucose levels and body weights were determined. In addition, OneTouch® Ultra™ blood glucose monitoring system (LifeScan Inc. 2005, California, USA) was used to measure the whole blood glucose

Correspondence to: Sirinush Sricharoenvej
E-mail: sissc@mahidol.ac.th

levels at 48 and 72 hours after the induction and before sacrifice. All animals were sacrificed at 24 weeks after the inductions as a long term.

Histological Study of Heart

All cardiac chambers were fixed with Bouin's solution. The standard procedures for histology processing were followed. The specimens were serially sectioned at 7 μm thick. After that, the serial sections were mounted on the glass slides, stained with hematoxylin and eosin, viewed and photographed under the LM (Axiostar plus, Jena, Germany), connected to a digital camera (AxioCam MRc, Jena, Germany).

Ultrastructures of Heart

Four cardiac chambers were processed for the conventional TEM. The blocks of each tissue were serially sectioned by an ultramicrotome (80-85 nm thick; Leic EM: UC6, Austria). Then, the sections were stained with uranyl acetate and lead citrate, observed and photographed under the TEM (JEOL JEM 1230, Japan).

Measurement in Diameters

Ten light micrographs were taken in each chamber of all rats. Both sizes of cardiac myocytes and Purkinje fibers were determined by using the digital image analysis with computer programs (AxioVision Rel. 4.6, Jena, Germany). The diameter of each cell was measured at three points. The first point was at the central part of the cell with a nucleus. The second and third points were at 10 μm intervals from each side of the first point. All points were calculated as an average of one cell.

Statistical Analysis

The results were expressed as means \pm standard deviations (SD). The comparisons were performed by using Mann-Whitney U test (SPSS 16.0 software). The significance level was set at p-value $<$.05.

RESULTS

In the diabetic rats as in the previous study,⁵ urine glucose levels were more than 500 mg/dL, and whole blood glucose levels were greater than 300 mg/dL. Moreover, body weight significantly decreased (289.27 ± 64.62 g), when compared to that in the control rats (444.83 ± 42.02 g, $p <$.05).

Each chamber consisted of three layers; endocardium, myocardium, and epicardium. Alterations of cells and their ultrastructures of each layer in all chambers were similar appearances. When compared to those in the control, diabetic endothelial and mesothelial cells were swollen and the subendocardial/subepicardial layers revealed thickening with fibrosis (Fig 1A-D). In the diabetic cardiac myocytes,

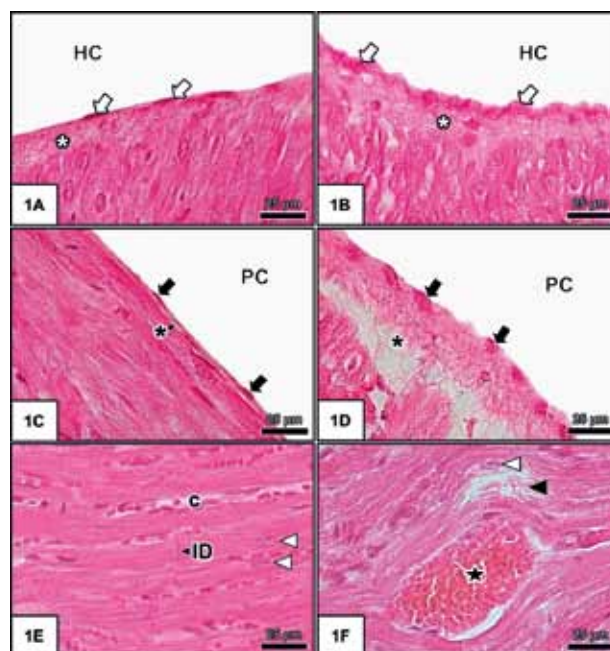


Fig 1. Light micrographs of three layers in cardiac control (1A, 1C, 1E) and DM (1B, 1D, 1F): endocardium (1A-B), epicardium (1C-D), myocardium (1E-F). Endothelial cells (white arrows), subendocardial layers (white asterisks), heart cavity (HC), mesothelial cells (black arrows), subepicardial layers (black asterisks), pericardial cavity (PC), cardiac nuclei (white arrowheads), intercalated disc (ID), capillary (c), disorganization of cardiac myofibrils (black arrowheads), interstitial hemorrhage (a black star). Hematoxylin and eosin staining.

they were hypertrophy with disorganization of myofibrils. Furthermore, diabetic myocardium of left ventricle displayed extensive interstitial hemorrhage (Fig 1E-F, Table 1). In the diabetic myocardium, interstitial fibrosis, infiltrations of lymphocytes and macrophages, and contraction band necrosis were examined. The diabetic Purkinje fibers were significantly larger than those in control, and their myofibrils were disorganized (Fig 2A-E, Table 1).

Under the TEM, swollen endothelial/mesothelial cells in the DM laid on thick basal lamina, and their cytoplasm contained numerous pinocytotic vesicles, vacuoles, and dilated rER. Their nuclei were irregular shape with invaginations of nuclear membrane. The subendocardial/subepicardial layers were enlarged with accumulation of collagen fibrils (Fig 3A-D). The arrangements of sarcomere were irregular and myofilaments were lost. Interestingly, number of specific atrial granules decreased in the diabetic atrial cardiac myocytes (Fig 3E-F). Additionally, there were increased invaginations of cardiac nuclei and thickening of heterochromatin lining nuclear membrane in the ven-

TABLE 1. Comparisons in diameters of cardiac myocytes and Purkinje fibers in control and DM.

Groups	Diameters of cardiac myocytes (μm)		Diameters of Purkinje fibers (μm)	
	Control (n=90)	DM (n=120)	Control (n=90)	DM (n=120)
Right atrium	16.97 \pm 0.64	21.78 \pm 0.91*	-	-
Right ventricle	19.89 \pm 0.31	22.81 \pm 0.32*	43.31 \pm 0.78	49.28 \pm 1.38*
Left atrium	17.96 \pm 1.68	22.39 \pm 0.94*	-	-
Left ventricle	21.55 \pm 0.72	23.89 \pm 1.01*	42.31 \pm 2.40	48.75 \pm 1.49*

*p-value $<$.05 compared to the same chamber of the age-matched control rats

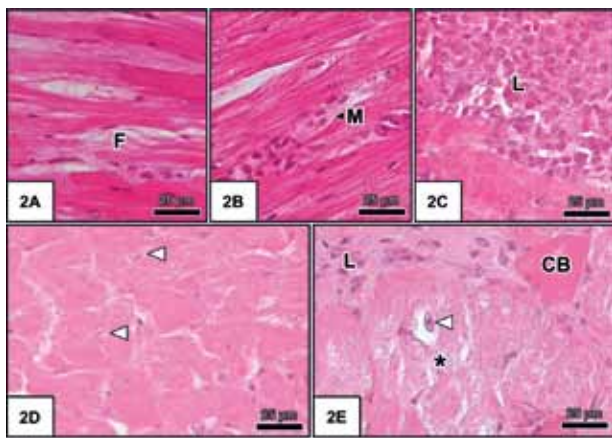


Fig 2. Light micrographs of diabetic myocardium (2A-C), Purkinje fibers of control (2D) and DM (2E). Interstitial fibrosis (F), macrophage (M), lymphocyte infiltration (L), Purkinje fibers (white arrowheads), disorganization of Purkinje fiber (a black asterisk), contraction band necrosis (CB). Hematoxylin and eosin staining.

tricular cardiac myocytes (Fig 4A-B). Some diabetic cardiac myocytes exhibited contraction band necrosis, increased number of swollen mitochondria with disrupted cristae, numerous lipid droplets and myelin figures (Fig 4C-D). The intercalated disc was damaged in some portions (Fig 4E-F). The modifications of diabetic Purkinje fibers were

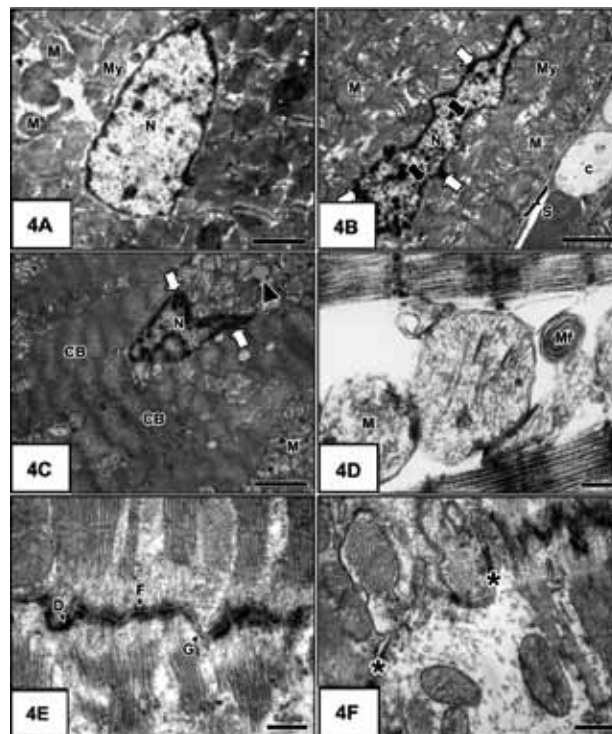


Fig 4. Transmission electron micrographs of myocardium in control (4A, E) and diabetic (4B-D, F) rats. Nuclei (N), mitochondria (M), myofilament (My), capillary (c), sarcomere (S), thick heterochromatin (white arrows), invagination of nuclear membrane (black arrows), contraction band necrosis (CB), lipid droplet (a black arrowhead), myelin figure (Mf), desmosome (D), fascia adherens (F), gap junction (G), disrupted intercalated disks (black asterisks).

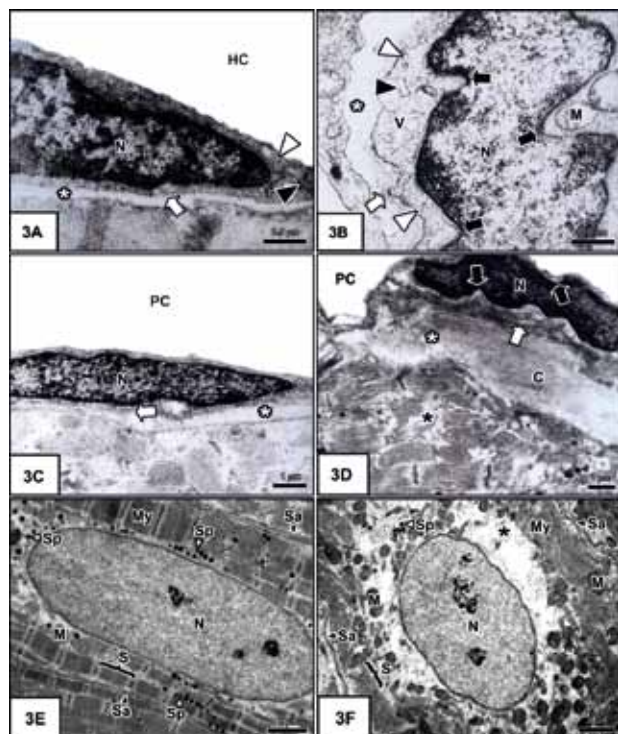


Fig 3. Transmission electron micrographs of three layers in cardiac control (3A, 3C, 3E) and DM (3B, 3D, 3F): endocardium (3A-B), epicardium (3C-D), myocardium (3E-F). Nuclei (N), rER (black arrowheads), pinocytotic vesicles (white arrowheads), subendocardial/subepicardial layers (white asterisks), basal lamina (white arrows), invagination of nuclear membrane (black arrows), mitochondria (M), vacuole (V), heart cavity (HC), pericardial cavity (PC), collagen fibrils (C), myofilament (My), sarcomere (S), loss of myofilament (a black asterisk), specific atrial granules (Sp), sarcolemma (Sa).

destroyed cristae in mitochondria and disorganization of sarcomere (Fig 5A-B). The diabetic endothelial cells of capillary swelled and protruded into lumen (Fig 5C-D). The large numbers of pinocytotic vesicles and vacuoles were found in their cytoplasm. Close contact between pericytes and capillary endothelial cells lost, because of thick basal lamina (Fig 5E-F).

DISCUSSION

In this study, increases in diameters of both cardiac myocytes and Purkinje fibers were found in the diabetic rats. The hypertrophy of these might probably represent a compensatory mechanism in the adaptation of cardiac function in hyperglycemia of diabetic stress.⁶ Furthermore, hypertrophy of cardiac myocytes was due to swollen mitochondria and increases in numbers of mitochondria, lipid droplets, and myelin figures. Both raised reactive oxygen species (ROS) and fatty acid during DM lead to swelling of mitochondria via a loss of membrane permeability.⁷ Moreover, ROS induces phospholipid cardiolipin in the inner membrane of mitochondria that interacts with ROS to disrupt the cristae.⁸ Risen number of mitochondria associates with mitochondrial biogenesis during the diabetes such as hypoxia, ischemia and cardiac failures.⁹ Damaged organelle such as mitochondria are fused by lysosomes in autophagy and finally become myelin figures.¹⁰ In ketone acidosis during the diabetes, reduced activity of carnitine acyl transferase and transportation of fatty acyl-CoA into the mitochondria cause formation of lipid droplets in the

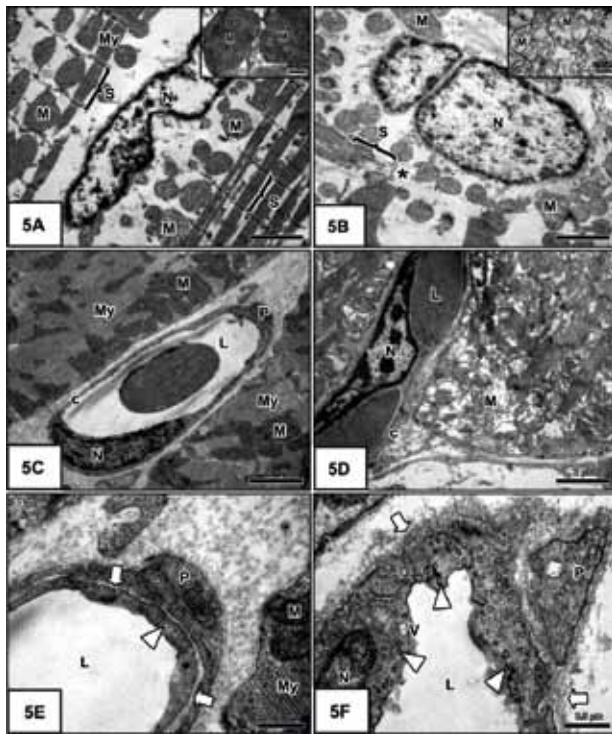


Fig 5. Transmission electron micrographs of Purkinje fibers in control (5A) and diabetic (5B) rats, and capillary of control (5C, 5E) and diabetic (5D, 5F) rats. Nuclei (N), mitochondria (M), myofilament (My), sarcomere (S), disorganization of sarcomere (a black asterisk), capillary (c), pericyte (P), lumen of capillary (L), pinocytotic vesicles (white arrowheads), basal lamina (white arrows), vacuole (V).

cytoplasm of diabetic myocardium.¹¹ Although the diameter of Purkinje fibers increased in the diabetic stage, they were partially intact. Normally, higher activity of glucose-6-phosphate dehydrogenase in the conducting system produces an antioxidant, glutathione, to protect Purkinje fibers during increased ROS in DM.¹² In the DM, cardiac myocytes and Purkinje fibers became disorganization and loss of myofibrils. Lower levels of cardiac specific transcription factor and myosin Ca^{2+} ATPase in the diabetes cause diminished alpha-myosin heavy chain expression and myosin light chain phosphorylation. Moreover, -actin mRNA decreases in the cardiac diabetic rats that causes reduction of F-actin.¹³ Furthermore, there is decreased connexin 43 in the intercalated disc of diabetic myocardium.³ As a consequence, disruption of intercalated disc occurred in DM that increases an incident of cardiac arrhythmia.⁴ Moreover, there were contraction band necroses in the diabetic myocardium. In calcium-independent mechanism, adenosine triphosphate synthesis is low in the STZ-diabetic rats and activates hypercontraction of sarcomere.¹⁴ In the oxidative stress, activated caspase 6 leads to disassembly of nuclear membrane with raised numbers of cell organelle as mentioned above that may cause an invagination of nuclear membrane. Because of DNA cleavage by endonuclease during DM, thick heterochromatin occurred in the cardiac myocytes.¹⁵ Additionally, contraction and relaxation of ventricles are stronger than those of atrium.¹⁶ As a result, increases in number of heterochromatin in nucleus and invagination of nuclear membrane were found only in the ventricular cardiac myocytes. Decreased number of specific atrial granules as in this investigation is due to increased secretion, decreased synthesis and mRNA expression of

atrial natriuretic peptide in the STZ-induced diabetic rats.¹⁷ During the diabetes, advance glycation end product is produced and acts as a chemotactic factor for macrophages that secrete cytokines to attract inflammatory cells such as lymphocytes.¹⁸ Therefore, lymphatic infiltration was observed in this examination. It was found that fibrosis happened in the subendocardial and subepicardial layers as well as pericapillary. High glucose level activates gene enhancer sequence of the collagen promoter. Then, fibroblasts synthesize and secrete collagen fibril accumulation.¹⁹ Moreover, numerous pinocytotic vesicles and vacuoles as well as rER dilatation were investigated in the cytoplasm of endothelial and mesothelial cells. The raised pinocytotic vesicles are cause of increased numbers of low density lipoprotein (LDL) and oxidation of LDL (oxLDL) in the diabetic stage. The oxLDL leads to an increased ruffling of plasma membrane and numerous pinocytotic vesicles in cultured vascular endothelial cells.²⁰ Because of high level of ROS, endothelial dysfunction is associated with damaged mitochondria, which are digested by autophagy.²¹ Accordingly, the vacuoles were observed in the diabetic rats. Moreover, dilatation of rER was found in endothelial/mesothelial cells due to hyperfunction of rER to synthesize more proteins for mitochondrial duplication and enzymes for lysosome activity. In addition, an increased fatty acid in the diabetes incorporates into biological membrane of rER that contributes to rER dilatation.²² The swollen endothelial cells of capillary caused a narrow lumen in the diabetic group. Due to thick basal lamina, contact between pericyte and capillary endothelial cell was widened. As a result, blood supply of heart reduces that contributes ischemic heart failure in the diabetic patients.²³ Moreover, severe diabetic damage of left ventricular chamber was indicated by interstitial hemorrhage. Increased expression of matrix metalloproteinase (MMP), an enzyme for tight junction degradation, in endothelial cells of the diabetic retina occurs.²⁴ Therefore, disruption of tight junction between endothelium in capillary happens. This mechanism causes capillary aneurysm in the diabetic heart.²⁵ Because of the highest blood pressure in the left ventricle and destroyed endothelium of capillary, the hemorrhage into the interstitial space is detected only in this chamber.

In conclusion, numerous alterations in all chambers of heart in developing cardiac failure in DM were shown. Consequently, the present study provides an important basic knowledge to understand the pathological changes and further therapeutic treatment of cardiac complications in the DM patients.

ACKNOWLEDGMENTS

This research was supported by Siriraj Graduate Thesis Scholarship 2008 and Chalermprakiat Grant, Faculty of Medicine Siriraj Hospital, Mahidol University.

REFERENCES

1. Bauters C, Lamblin N, Mc Fadden EP, Van Belle E, Millaire A, de Groote P. Influence of diabetes mellitus on heart failure risk and outcome. *Cardiovasc Diabetol.* 2003 Jan;2(1):1-16.
2. Nemoto O, Kawaguchi M, Yaoita H, Miyake K, Maehara K, Maruyama Y. Left ventricular dysfunction and remodeling in streptozotocin-induced diabetic rats. *Circ J.* 2006 Mar;70(3):327-34.

3. Howarth FC, Chandler NJ, Kharche S, Tellez JO, Greener ID, Yamanushi TT, et al. Effects of streptozotocin-induced diabetes on connexin 43 mRNA and protein expression in ventricular muscle. *Mol Cell Biochem.* 2008 Dec;319(1-2):105-14.
4. Movahed MR. Diabetes as a risk factor for cardiac conduction defects: a review. *Diabetes Obes Metab.* 2007 May;9(3):276-81.
5. Sricharoenvej S, Boonprasop S, Lanlua P, Piyawinijwong S, Niyomchan A. Morphological and microvascular changes of the adrenal glands in streptozotocin-induced long-term diabetic rats. *Ital J Anat Embryol.* 2009 Jan-Mar;114(1):1-10.
6. Aragno M, Mastrocola R, Medana C, Catalano MG, Vercellinato I, Danni O, et al. Oxidative stress-dependent impairment of cardiac-specific transcription factors in experimental diabetes. *Endocrinology.* 2006 Dec;147(12):5967-74.
7. Oliveira PJ. Cardiac mitochondrial alterations observed in hyperglycaemic rats—what can we learn from cell biology? *Curr Diabetes Rev.* 2005 Feb;1(1):11-21.
8. Dabkowski ER, Williamson CL, Bukowski VC, Chapman RS, Leonard SS, Peer CJ, et al. Diabetic cardiomyopathy-associated dysfunction in spatially distinct mitochondrial subpopulations. *Am J Physiol Heart Circ Physiol.* 2009 Feb;296(2):H359-69.
9. Shen X, Zheng S, Thongboonkerd V, Xu M, Pierce WM Jr, Klein JB, et al. Cardiac mitochondrial damage and biogenesis in a chronic model of type 1 diabetes. *Am J Physiol Endocrinol Metab.* 2004 Nov; 287(5): E896-905.
10. Giacomelli F, Wiener J. Primary myocardial disease in the diabetic mouse. An ultrastructure study. *Lab Invest.* 1979 Apr;40(4):460-73.
11. Reinila A, Akerblom HK. Ultrastructure of heart muscle in short-term diabetic rats: influence of insulin treatment. *Diabetologia.* 1984 Sep;27(3):397-402.
12. Kuroda A, Saito K, Tanaka H. Histochemical studies on the conduction system of diabetic rat hearts. *Arch Histol Cytol.* 1990 May;53(2):193-8.
13. Depre C, Young ME, Ying J, Ahuja HS, Han Q, Garza N, et al. Streptozotocin-induced changes in cardiac gene expression in the absence of severe contractile dysfunction. *J Mol Cell Cardiol.* 2000 Jun;32(6):985-96.
14. Tanaka Y, Konno N, Kako KJ. Mitochondrial dysfunction observed in situ in cardiomyocytes of rats in experimental diabetes. *Cardiovasc Res.* 1992 Apr;26(4):409-14.
15. Brodie C, Blumberg PM. Regulation of cell apoptosis by protein kinase C delta. *Apoptosis.* 2003 Jan;8(1):19-27.
16. Guyton AC, Hall JE. *Textbook of medical physiology.* 11th rev. ed. Philadelphia: Elsevier Saunders; 2006. p.103-15.
17. Wu SQ, Kwan CY, Tang F. Streptozotocin-induced diabetes has differential effects on atrial natriuretic peptide synthesis in the rat atrium and ventricle: a study by solution-hybridization-RNase protection assay. *Diabetologia.* 1998 Jun;41(6):660-5.
18. Hudson BI, Hofmann MA, Bucciarelli L, Wendt T, Moser B, Lu Y, et al. Glycation and diabetes: The RAGE connection. *Curr Sci.* 2002 Dec;83(12):1515-21.
19. Asbun J, Villarreal FJ. The pathogenesis of myocardial fibrosis in the setting of diabetic cardiomyopathy. *J Am Coll Cardiol.* 2006 Feb;47(4):693-700.
20. Chow SE, Lee RS, Shih SH, Chen JK. Oxidized LDL promotes vascular endothelial cell pinocytosis via a prooxidation mechanism. *FASEB J.* 1998 Jul;12(10):823-30.
21. Popov D, Sima A, Stern D, Simionescu M. The pathomorphological alterations of endocardial endothelium in experimental diabetes and diabetes associated with hyperlipidemia. *Acta Diabetol.* 1996 Mar;33(1): 41-7.
22. Waters PJ, Flynn MD, Corral RJ, Pennock CA. Increases in plasma lysosomal enzymes in type 1 (insulin-dependent) diabetes mellitus: relationship to diabetic complications and glycaemic control. *Diabetologia.* 1992 Oct;35(10):991-5.
23. Das SR, Drazner MH, Yancy CW, Stevenson LW, Gersh BJ, Dries DL. Effects of diabetes mellitus and ischemic heart disease on the progression from asymptomatic left ventricular dysfunction to symptomatic heart failure: a retrospective analysis from the studies of left ventricular dysfunction (SOLVD) prevention trial. *Am Heart J.* 2004 Nov;148(5):883-8.
24. Giebel SJ, Menicucci G, McGuire PG, Das A. Matrix metalloproteinases in early diabetic retinopathy and their role in alteration of the blood-retina barrier. *Lab Invest.* 2005 May;85(5):597-607.
25. Seitz S, Syed Ali S, Stroder D. Angioarchitecture in the heart of rats with streptozotocin-induced diabetes mellitus. *Ann Anat.* 1993 Jun;175(3):285-9.